Supporting Information of:

Absolute configuration determination of SMTP-7 via microcrystal electron diffraction (MicroED)

Material and Characterizations

The SMTP-7 and SMTP-7D samples were obtained from TMS Co., Ltd. Both samples were used for MicroED data collection and VCD analysis directly without further purification.

Optical microscopic images were acquired using an Olympus BX51 microscope (Olympus Corp, Japan) equipped with a QImaging Micropublusher 5.2 RTV camera (QImaging, Inc., Canada), and imaging capturing and processing software QCapture Pro. As shown in **Figure S1**, both materials are fine birefringent powder. The crystal dimensions are on the order of 1-10 micron.
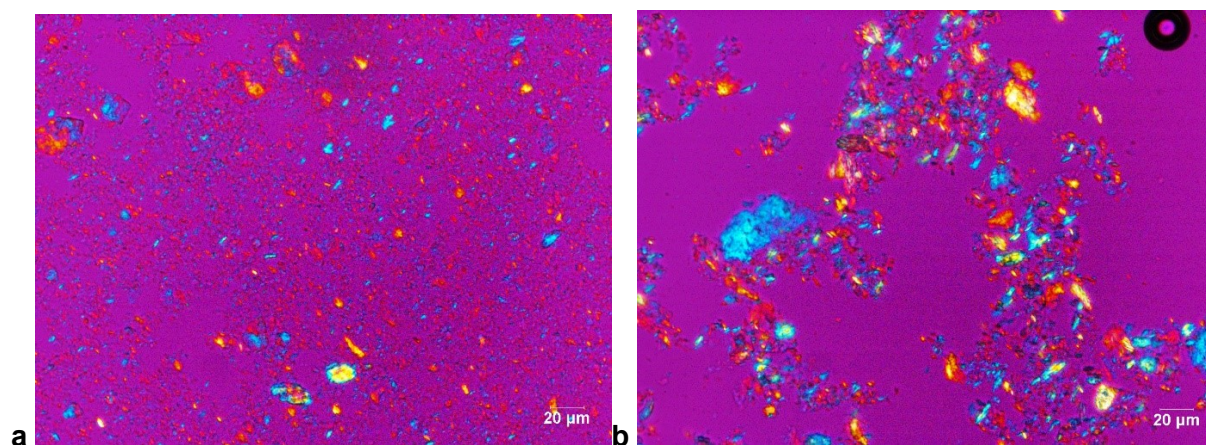

Figure S1. PLM images of the crystalline samples: (a) SMTP-7 samples, (b) SMTP-7D samples. Both samples were directly used for MicroED data collection.

Crystallinity of the samples was studied using D8 ADVANCE X-ray powder diffractometer using Cu Ka radiation (Bruker, Madison, WI). The instrument is equipped with a long fine focus X-ray tube. Diffracted radiation was detected by a LYNXEYE (1D mode) detector. A 2θ continuous scan from 3.0° to 40.0° at 0.01° increment was taken with a 3.0 sec exposure time. The samples were measured using a zero-background plate. The calculated X-ray powder diffraction (XRPD) patterns were calculated from the MicroED structures using Mercury 4.3.0. As shown in **Figure S2**, both materials are crystalline. The experimental patterns are in good match with calculated XRPD pattern, although a unit cell expansion from 80K to 290K should be accounted for the slight mismatch between the calculated and experimental patterns.
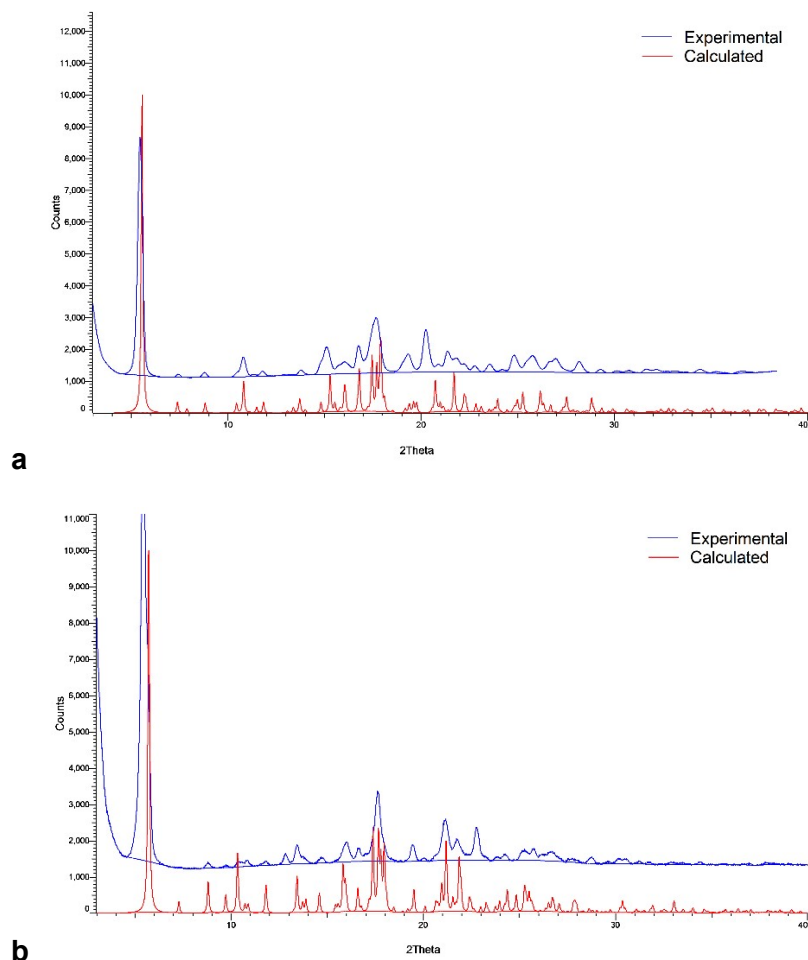
Figure S2. Experimental (ambient) and calculated (80 K) XRPD patterns of (a) SMTP-7, (b) SMTP-7D.

MicroED Structure Determination

A small amount of SMTP-7 and SMTP-7D powdered material was applied to pure carbon grids (Ted Pella 01840), and the SMTP-7D grid was heated in a vacuum oven at 40°C for 15 minutes to remove volatile contaminants. MicroED data were collected as previously described using a Thermo Fisher Glacios Cryo Transmission Electron Microscope equipped with a CETA-D detector[1,2]. Datasets were indexed, refined, integrated and scaled using the program DIALS[3]. Datasets were collected using automated methods and the best datasets were combined to increase completeness and redundancy. Xia2 was used to convert file types[4] and XPREP[5] was used to analyze possible space groups. The data were phased by dual space methods with SHELXD[6]. Kinematical refinement was carried out using SHELXL[7] as implemented in Olex2[8] and validation was carried out in PLATON[9]. Due to the low resolution of the data, many restraints were employed to idealize the structures. The final SMTP-7 and SMTP-7D structures and reduced reflections can be accessed from the CCDC (deposition number: 2208429 and 2208444). Selected crystallographic data is summarized in **Table S1**. Based on the structures, the XRPD pattern was calculated as shown in **Figure S2**.

Data Collection, Reduction and Refinement Information		
	SMTP-7	**SMTP-7D**
Data Collection		
Wavelength (Å)	0.02501 (electrons)	
Temperature (°C)	-193	
Camera length (mm)	1100	
Oscillation per frame (°)	0.89	
Dose per degree ($e^-/Å^2$)	~0.028	
Data Reduction		
Space group	$P2_12_12$	$P2_12_12_1$
Number of datasets comb.	26	4
Unit cell lengths a, b, c (Å)	12.897(3), 31.766(6), 11.213(2)	11.238(2), 13.188(3), 30.929(6)
angles α, β, γ (°)	90, 90, 90	90, 90, 90
Resolution (Å)	12.77 - 0.90	13.19 - 1.00
Total Reflections	180575	40924
Unique Reflections	3222	2234
Multiplicity	56.04	18.3
Completeness (%)	85.90	81.5
$I/\sigma(I)$	6.3	7.7
R_{meas}[#]	0.47	0.20
R_{pim}[#]	0.06	0.06
$CC_{1/2}$	0.997	1.00
Refinement		
Chemical Formula	$C_{51}H_{68}N_2O_{10}$	$C_{51}H_{68}N_2O_{10}$
Z	4	4
Z'	1	1
Data | Restraints | Param.	5710 | 614 | 437	3965 | 408| 581
R_1 | wR_2 for I≥2σ(I)	16.19% | 37.86%	14.54% | 34.58%
R_1 | wR_2 for all data	26.61% | 40.95%	18.80% | 36.75%
GooF (Goodness of Fit)	0.984	1.206
Largest diff. peak/hole ($eÅ^{-3}$)	0.18 | -0.26	0.19 | -0.12

Table S1. Crystallographic data summary for MicroED structures of SMTP-7 and SMTP-7D. [#]R_{meas} and R_{pim} were calculated without combining Friedel pairs (I+/-)
Check cif response for the SMTP-7 structure:

PROBLEM: The value of Rint is greater than 0.25
RESPONSE: This is a MicroED dataset, which in general, has higher Rint value.

PROBLEM: The Value of Rint is Greater Than 0.12 ....   0.378 Report
RESPONSE: This is a MicroED dataset, which in general, has higher Rint value.

PROBLEM: Too many H on C in C=N Moiety in Main Residue ..   C1C Check
RESPONSE: The C1C carbon is originated from l-ornithine, which is certainly sp3 hybridized, thus two hydrogens are expected

PROBLEM: Short Intra XH3 .. XHn   H19B   ..H24B   .   1.25 Ang.
RESPONSE: This is on the long alkyl group, where the methylene and methyl have space to rotate. The position of all the hydrogens on the alkyl groups were refined as the same riding models, to keep consistent, this pair of hydrogens were not forced away.

PROBLEM: The value of sine(theta_max)/wavelength is less than 0.575
RESPONSE: The ED dataset has weak intensities for higher resolution reflections.

PROBLEM: High R1 Value ....   0.16 Report
RESPONSE: This is a MicroED dataset, which in general, has higher R1 value, partially due to only kinematically refined.

PROBLEM: High wR2 Value (i.e. > 0.25) ....   0.41 Report
RESPONSE: This is MicroED dataset, which in general, has higher wR2 value, partially due to only kinematically refined.

PROBLEM: Hirshfeld Test Diff for   C9A   --C25A   .   7.5 s.u.
RESPONSE: The anisotropic displacement parameter of these atoms are treated slightly different with SUMP and EADP constraints in different sets of atoms to make chemical sense.

PROBLEM: D-H Bond Without Acceptor O8C   --H8C   .   Please Check
RESPONSE: Hydrogen bonds is not observed for the carboxylic acid.

PROBLEM: The Embedded .res File Includes a DAMP Command .   100.0 Report
RESPONSE: This is necessary to keep the model convergent.

Check cif response for the SMTP-7D structure:

PROBLEM: The value of sine(theta_max)/wavelength is less than 0.550
RESPONSE: This is a MicroED dataset, which has weak intensities at high angle.

PROBLEM: The value of Rint is greater than 0.18
RESPONSE: This is a MicroED dataset, which in general, has higher Rint value.

PROBLEM: The Value of Rint is Greater Than 0.12 .... 0.191 Report
RESPONSE: This is a MicroED dataset, which in general, has higher Rint value.

PROBLEM: High wR2 Value (i.e. > 0.25) .... 0.37 Report
RESPONSE: This is a MicroED dataset, which in general, has higher wR2 value.

PROBLEM: Low Bond Precision on C-C Bonds .... 0.0398 Ang.
RESPONSE: Due to the high Rint and weak overall intensities, lower bond precision is not surprising.

PROBLEM: Short Inter H...H Contact H8B   ..H15A   .   1.99 Ang.
RESPONSE: The hydrogens are refined as riding model, not forced to be away from each other.

PROBLEM: Short Intra XH3 .. XHn   H15B   ..H24A   .   1.77 Ang.
RESPONSE: The hydrogens are refined as riding model, not forced to be away from each other.

PROBLEM: Short Inter XH3 .. XHn   H18A   ..H22E   .   1.91 Ang.
RESPONSE: The hydrogens are refined as riding model, not forced to be away from each other.

PROBLEM: Short Inter D-H..H-X   H23E   ..H27B   .   1.96 Ang.
RESPONSE: The hydrogens are refined as riding model, not forced to be away from each other.

PROBLEM: Short Inter D-H..H-X   H25A   ..H25B   .   1.96 Ang.
RESPONSE: The hydrogens are refined as riding model, not forced to be away from each other.

PROBLEM: D-H Bond Without Acceptor O7C   --H7C   .   Please Check
RESPONSE: There is no hydrogen bonding for this carboxylic acid group.

PROBLEM: D-H Bond Without Acceptor O26A   --H26A   .   Please Check
RESPONSE: There is no nearby acceptor available.

VCD measurement and calculation

VCD spectrum of SMTP-7 was collected in d_6-DMSO solution, using ChiralIR w/DualPEM spectrometer. A total measurement time of 24 hour was applied with resolution of 4 cm^{-1}. As shown in **Figure S3**, two VCD calculation methodologies were implemented. The calculated VCD result shown in the **Figure S3(a)** is based on a direct optimization and frequency calculation from the MicroED structure of SMTP-7, at level of 6-31G(d)/B3LYP/CPCM(DMSO), using Gaussian 16. The calculated VCD result shown in the **Figure S3(b)** is based on an addition of VCD spectra calculated from two simplified pieces (shown in **Figure S3c**). The VCD spectra of the two fragments were calculated at the same level of 6-31G(d)/B3LYP/CPCM (DMSO), using a weighted combination of VCD spectra calculated from a total number of 456 Boltzmann distributed conformers.

Although the VCD peaks do not fit well in the lower frequency region for the first method, the two VCD peaks around 1700cm^{-1} which involve carbonyl stretching shows a clear agreement with the αS assignment. Furthermore, the second method offers a much better fit for the low frequency region which further support our absolute configuration assignment of SMTP-7.
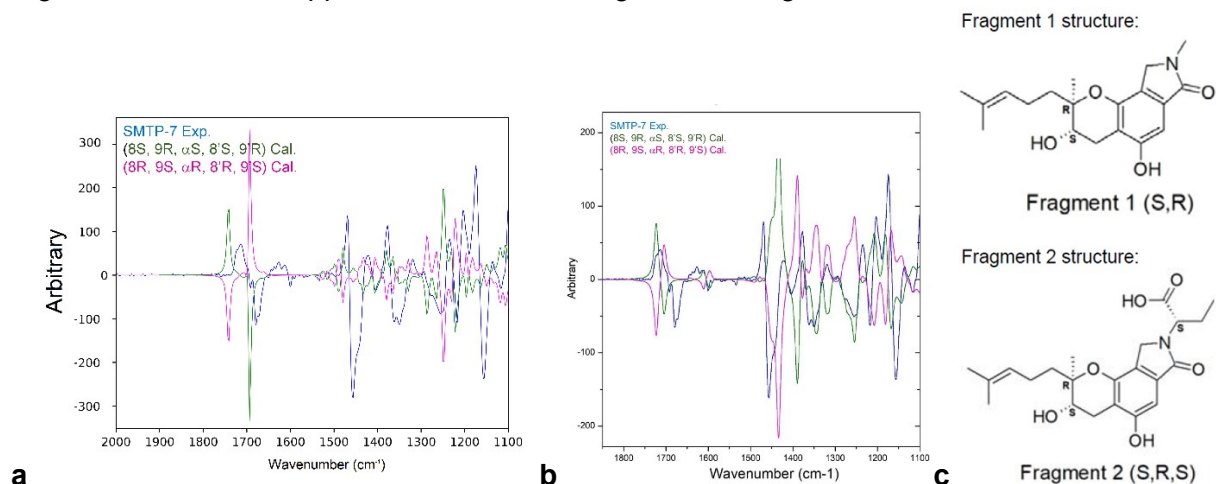

Figure S3. (a,b) Experimental and calculated VCD spectra of SMTP-7 with two computational methodologies. **(c)**, Fragments structure for the second computational method.

Dynamical refinement

The datasets of both samples that were used in the kinematical refinement were converted from .img files to .tif files using a python script, kindly provided by Dr. Paul Klar at FZU Palatinus Group. The image files of each individual dataset were then reprocessed with PET2 Version 2.1.20210323[9]. In the reprocessing, a pts2 file was first created to import the dataset with λ = 0.025010, Å/pixel =0.00105036. The noise parameters were set to 10.0, 4.80, which should be carefully treated to enable a successful indexing and integration process. The max d* for integration and peak search were, in general, set at 0.8 $Å^{-1}$, which were modified if the dataset has much stronger or weaker reflection at high resolution. For weaker datasets, later frames showed very weak reflections, therefore the latter portion of many datasets was discarded. Beam

stop was drawn in each run, and the beam center was adjusted for each individual frame via Friedel pairs, with reflections of I/sigma > 20 being considered. Rotation axis was then refined, which is typically a small number close to 0 deg. Frames were indexed and the unit cells were refined as orthorhombic cells. The RC width was set at 0.001 Å^{-1} and the apparent mosaicity was set to 0.1 deg. The orientation angles and centers of each frame were then refined using frame simulation. Finally, the frames were integrated with dynamical refinement to generate the cif_pets file, using virtual frames setting with number of frames = 4 and step = 2.

The dynamical refinement was conducted using Jana2020[10,11], version 22Mar2021. First the integrated reflection was loaded with default settings, then the kinematically refined final MicroED structures (cif files) of SMTP-7 and SMTP-7D were loaded. Default parameters for ED were used except max diffraction vector = 0.6 Å^{-1} max f and Dsg(min) = 0.001. The thickness of each frame was then optimized in rotation geometry. In the actual dynamical refinement, all structural parameters were fixed, using the dynamical LS method, each run was refined against F(obs) to convergent to acquire the R-factors. To generate the enantiomer, the "change enantiomorph" in Jana2020 was used, and the refinement was performed from re-optimization of the thickness in each frame. As shown in **Table S2**, the wR2(all) of correct absolute configuration is always lower than the inverted model in all cases.

	wR2 correct abs. conf.	wR2 enantiomer	% Difference
SMTP-7	0.1951	0.2086	6.47
	0.1921	0.2133	9.94
	0.2088	0.2224	6.12
	0.1924	0.2162	11.01
	0.1769	0.1945	9.05
	0.1921	0.2268	15.30
	0.1562	0.1855	15.80
	0.1476	0.1696	12.97
	0.1723	0.2173	20.71
	0.1842	0.2015	8.59
SMTP-7D	0.2291	0.2304	0.56
	0.2245	0.2453	8.48
	0.2329	0.2495	6.65
	0.2172	0.2394	9.27

Table S2. R-factor comparison for the enantiomeric solutions of SMTP-7 and SMTP-7D

Reference

[1]   J. F. Bruhn, G. Scapin, A. Cheng, B. Q. Mercado, D. G. Waterman, T. Ganesh, S. Dallakyan, B. N. Read, T. Nieusma, K. W. Lucier, M. L. Mayer, N. J. Chiang, N. Poweleit, P. T. McGilvray, T. S. Wilson, M. Mashore, C. Hennessy, S. Thomson, B. Wang, C. S. Potter, B. Carragher, Front. Mol. Biosci. **2021**, 8, 354.

[2]   A. Cheng, C. Negro, J. F. Bruhn, W. J. Rice, S. Dallakyan, E. T. Eng, D. G. Waterman, C. S. Potter, B. Carragher, Protein Sci. Publ. Protein Soc. **2021**, 30, 136–150.

*[3]   M. T. B. Clabbers, T. Gruene, J. M. Parkhurst, J. P. Abrahams, D. G. Waterman, Acta Crystallogr. Sect. Struct. Biol. **2018**, 74, 506–518.*

*[4]   G. Winter, J. Appl. Crystallogr. **2010**, 43, 186–190.*

*[5]   Sheldrick, G.M. (2008) XPREP Version 2008/2. Bruker AXS Inc., Madison., **n.d.***

*[6]   T. R. Schneider, G. M. Sheldrick, Acta Crystallogr. D Biol. Crystallogr. **2002**, 58, 1772–1779.*

*[7]   G. M. Sheldrick, Acta Crystallogr. Sect. C Struct. Chem. **2015**, 71, 3–8.*

*[8]   O. V. Dolomanov, L. J. Bourhis, R. J. Gildea, J. A. K. Howard, H. Puschmann, J. Appl. Crystallogr. **2009**, 42, 339–341.*

*[9]   L. Palatinus, P. Brázda, M. Jelínek, J. Hrdá, G. Steciuk, M. Klementová, Acta. Crystallogr. B. Struct. Sci. Cryst. Eng. Mater. **2019**, 75, 512–522.*

[10]   *V. Petříček, V, M. Dušek, L. Palatinus. Z. Kristallogr. Cryst. Mater. **2014**, 229, 345–352.*

[11]   *L. Palatinus, V. Petříček, C. A. Corrêa, Acta Crystallogr. A: Found. Adv. 2015, 71, 235–244.*